atoms

MDPI

Article

Invariant Approach to the Interaction Between Several Fields and an Atom

Marco A. García-Márquez, Irán Ramos-Prieto and Héctor M. Moya-Cessa *

Instituto Nacional de Astrofísica, Óptica y Electrónica, Calle Luis Enrique Erro No. 1, Santa María Tonantzintla, Puebla 72840, Mexico; marcoa.garcia@inaoep.mx (M.A.G.-M.); iran@inaoep.mx (I.R.-P.)
* Correspondence: hmmc@inaoep.mx

Abstract

We present a general procedure to describe the dynamics of N degenerate quantized fields interacting resonantly with a two–level atom, all coupled with the same strength, within the rotating–wave approximation. Starting from the analysis of the two and three field cases, we generalize the method by identifying dynamical invariants that lead to a factorized form of the time–evolution operator. A unitary transformation reduces the problem to an effective Jaynes–Cummings Hamiltonian, where only one field interacts with the atom and the remaining modes contribute as free fields. Assuming initially coherent fields and an atomic superposition, we compute the atomic inversion and the mean photon number, revealing vacuum Rabi oscillations with a frequency determined by an effective coupling constant that exceeds the individual atom–field coupling, as well as the characteristic collapse–revival behavior.

Keywords: multimode Jaynes–Cummings model; dynamical invariants; vacuum Rabi oscillations; collapse and revival phenomena

1. Introduction

The interaction between atoms and quantized electromagnetic fields constitutes one of the fundamental pillars of quantum optics. The quantum Rabi model [1,2] describes the interaction between a two–level atom and a single quantized cavity mode. In the weak–coupling and near–resonant regime, the rotating–wave approximation allows one to neglect the counter–rotating terms, leading to the Jaynes–Cummings model [3–5], the most fundamental exactly solvable model capturing the essential physics of radiation-matter interaction, including spontaneous and stimulated emission, Rabi oscillations, the collapse–revival phenomenon [6,7], and the generation of nonclassical states of light, among others [8–11].

Over the years, these models have been generalized in several directions. For instance, the interaction with multiple atoms [12,13], described by the Dicke model [14,15] and its rotating–wave counterpart, the Tavis–Cummings model [16]. Other extensions consider atoms with N energy levels interacting with the field [17–19], or systems in which both the quantized field and the atom are influenced by an external classical field [20–22]. Generalized Jaynes–Cummings models have also been proposed to include intensity–dependent couplings [23] or multiphoton interactions between the field and the atom [24,25]. Moreover, time–dependent generalizations of the model have been considered [26].

Additionally, several studies have examined the interaction of a single two–level atom with multimode quantized fields [27,28], including analyses of systems involving two and

Check for updates

Academic Editor: Yew Kam Ho

Received: 27 November 2025
Revised: 29 December 2025
Accepted: 5 January 2026
Published: 8 January 2026

Copyright: © 2026 by the authors. Licensee MDPI, Basel, Switzerland. This article is an open access article distributed under the terms and conditions of the Creative Commons Attribution (CC BY) license.

three field modes coupled to the atom [29–31]. It has been shown, for instance, that the interaction of a two–level atom with two degenerate field modes can be mapped, through an appropriate symmetry transformation, onto an effective single–mode Jaynes–Cummings model, which admits an exact analytical solution [32,33]. Alternatively, the same system can be reduced to an effective one–quasi–mode Jaynes–Cummings model [29,34].

As part of the effort to explore multimode generalizations, in this work we describe a general procedure to analyze the dynamics of N degenerate quantized fields interacting resonantly with a two–level atom, all coupled with the same strength. In contrast to Ref. [35], where different coupling strengths were considered, we focus on the case of identical atom–field couplings, which enables a systematic generalization of the model. We first examine in detail the cases of two and three quantized fields interacting with the atom, from which the structure of the general method naturally emerges. We employ an operator approach based on the identification of dynamical invariants that provide a systematic way to construct the factorized form of the time–evolution operator. By applying a unitary transformation, we move to a reference frame in which only one field remains coupled to the atom, while the others contribute solely through their free–field Hamiltonians; that is, the resulting Hamiltonian corresponds to a Jaynes–Cummings model with an effective coupling constant larger than the individual one, plus the free–field terms of the decoupled modes. We then compute the atomic inversion and the time evolution of the mean photon number for one of the fields, assuming that the fields are initially in coherent states and the atom is prepared in a superposition state. The results exhibit vacuum Rabi oscillations with a frequency determined by the effective coupling constant, as well as the characteristic collapse and revival phenomena.

2. A Two–Level Atom Interacting with N Quantized Fields

Let us consider a single two–level atom interacting with N quantized electromagnetic modes, each confined in its own cavity and all sharing the same frequency. Each mode is coupled to the atom with identical strength, so that each atom–field pair is governed by a Jaynes–Cummings–type interaction within the rotating–wave approximation, as illustrated in Figure 1. The field modes do not interact among themselves; their only coupling is mediated through the single atom. Under these conditions, the dynamics of the atom–multimode field system is captured by the Hamiltonian [27] ($\hbar = 1$)

$$\hat{H} = \frac{\omega_0}{2}\hat{\sigma}_z + \omega_F \sum_{k=1}^{N} \hat{a}_k^\dagger \hat{a}_k + g\left(\hat{\sigma}_- \sum_{k=1}^{N} \hat{a}_k^\dagger + \hat{\sigma}_+ \sum_{k=1}^{N} \hat{a}_k\right), \tag{1}$$

where the k–th field mode, of frequency ω_F, is described by the annihilation and creation operators $\hat{a}_k$ and $\hat{a}_k^\dagger$. The operators $\hat{\sigma}_z$, $\hat{\sigma}_+$, and $\hat{\sigma}_-$ denote the usual Pauli matrices acting on the atomic two–level system, explicitly defined in terms of the excited and ground atomic states, $|e\rangle = [1,0]^T$ and $|g\rangle = [0,1]^T$ (where T denotes the transpose of the row vector), as

$$\hat{\sigma}_z = |e\rangle\langle e| - |g\rangle\langle g| = \begin{pmatrix} 1 & 0 \\ 0 & -1 \end{pmatrix}, \quad \hat{\sigma}_+ = |e\rangle\langle g| = \begin{pmatrix} 0 & 1 \\ 0 & 0 \end{pmatrix}, \quad \hat{\sigma}_- = |g\rangle\langle e| = \begin{pmatrix} 0 & 0 \\ 1 & 0 \end{pmatrix}, \tag{2}$$

and which obey the standard commutation relations $[\hat{\sigma}_z, \hat{\sigma}_\pm] = \pm 2\hat{\sigma}_\pm$ and $[\hat{\sigma}_+, \hat{\sigma}_-] = \hat{\sigma}_z$. The parameters ω_0 and g denote the atomic transition frequency and the atom–field coupling strength, respectively. It is worth noting that mode degeneracy can also occur in optical resonators supporting families of transverse modes, such as confocal or near–confocal cavities, where different Hermite–Gauss modes can share the same resonance frequency [36,37]. Thus, although the schematic configuration shown in Figure 1 is mainly conceptual, it

captures essential features of systems in which several degenerate or nearly degenerate modes interact with a single atom.

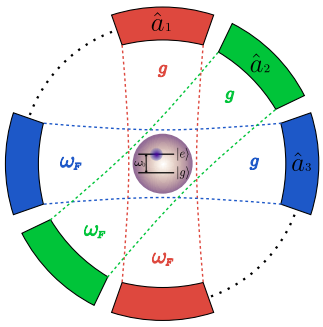


Figure 1. A two–level atom interacting with N quantized cavity field modes of equal frequency via identical Jaynes–Cummings couplings. The modes are mutually uncoupled and interact only through the atom.

Invariant Approach

In order to solve the dynamics of our system, we apply an invariant approach that allows us to factorize the evolution operator. Therefore, we look for operators that satisfy [38]

$$\frac{d\hat{I}}{dt} = \frac{\partial \hat{I}}{\partial t} - i\left[\hat{I}, \hat{H}\right] = 0. \tag{3}$$

Since the rotating–wave approximation is assumed, as in the Jaynes–Cummings model, the total number of excitations, denoted by $\hat{I}_1$, is conserved

$$\hat{I}_1 = \frac{\hat{\sigma}_z}{2} + \sum_{k=1}^{N} \hat{a}_k^\dagger \hat{a}_k. \tag{4}$$

It is straightforward to show that another invariant is

$$\hat{I}_2 = \frac{N}{2}\hat{\sigma}_z + \sum_{k=1}^{N} \hat{a}_k^\dagger \sum_{l=1}^{N} \hat{a}_l, \tag{5}$$

and it could be understood as representing the total number of excitations, but now considering a collective field mode. It is important to emphasize that, for the operator given in Equation (5) to be invariant, the fields must have the same frequency and identical coupling to the atom. It is also worth noting that the invariants $\hat{I}_1$ and $\hat{I}_2$ commute, that is, $[\hat{I}_1, \hat{I}_2] = 0$. Moreover, both invariants commute with each of the four explicit terms appearing in the Hamiltonian of Equation (1). This last property allows us to define the following operators

$$\hat{A}_N = \frac{\hat{\sigma}_+ \sum_{k=1}^{N} \hat{a}_k}{\sqrt{\hat{I}_2 + \frac{N}{2}}}, \qquad \hat{A}_N^\dagger = \frac{\hat{\sigma}_- \sum_{k=1}^{N} \hat{a}_k^\dagger}{\sqrt{\hat{I}_2 + \frac{N}{2}}}, \tag{6}$$

without ambiguity in the order of their factors, since the numerator and denominator commute. The operators thus defined satisfy the following commutation relations

$$[\hat{A}_N, \hat{A}_N^\dagger] = \hat{\sigma}_z, \qquad [\hat{A}_N, \hat{\sigma}_z] = -2\hat{A}_N, \qquad [\hat{A}_N^\dagger, \hat{\sigma}_z] = 2\hat{A}_N^\dagger, \tag{7}$$

that is, they close an algebra under the commutation operation. In terms of these constants of motion and operators, the Hamiltonian of the system, given in Equation (1), can be written as

$$\hat{H} = \frac{\Delta}{2}\hat{\sigma}_z + \omega_F \hat{I}_1 + g\sqrt{\hat{I}_2 + \frac{N}{2}}\left(\hat{A}_N^\dagger + \hat{A}_N\right), \tag{8}$$

where $\Delta = \omega_0 - \omega_F$ is the atom-field detuning. For simplicity, we consider the on–resonance case, for which the evolution operator corresponding to the Hamiltonian above can be written as

$$\hat{U}(t) = \exp\left(-i\omega_F \hat{I}_1 t\right) \exp\left(-igt\sqrt{\hat{I}_2 + \frac{N}{2}}(\hat{A}_N^\dagger + \hat{A}_N)\right), \tag{9}$$

where the factor $e^{-i\omega_F \hat{I}_1 t}$ only contributes an overall phase. We can apply the Wei–Norman theorem [39] to express the evolution operator in a factored form, as shown in Appendix A, to obtain

$$\hat{U}(t) = e^{-i\omega_F \hat{I}_1 t} e^{-i\tan\left(gt\sqrt{\hat{I}_2+\frac{N}{2}}\right)\hat{A}_N^\dagger} e^{\ln\left[\cos\left(gt\sqrt{\hat{I}_2+\frac{N}{2}}\right)\right]\hat{\sigma}_z} e^{-i\tan\left(gt\sqrt{\hat{I}_2+\frac{N}{2}}\right)\hat{A}_N}. \tag{10}$$

To establish a general procedure for determining the atomic inversion and the mean photon number in the case of a two–level atom interacting with N quantized field modes, we first analyze in detail the particular cases of $N = 2$ and $N = 3$, which provide the foundation for extending the method to the general case.

3. Two Quantized Fields Interacting with the Atom

First, we consider a two-level atom interacting with two quantized field modes. The corresponding Hamiltonian in this case is given by [29,35]

$$\hat{H} = \omega_F \hat{I}_1 + g\sqrt{\hat{I}_2 + 1}\left(\hat{A}_2 + \hat{A}_2^\dagger\right), \tag{11}$$

where the invariants given in Equations (4) and (5) are evaluated for $N = 2$. To obtain an evolution operator applicable to an initial condition, we move to a different reference frame, where the system is described by the state vector $|\varphi(t)\rangle$, through the following transformation

$$|\psi(t)\rangle = \hat{D}_{1-2}^\dagger(\theta)|\varphi(t)\rangle, \tag{12}$$

where $\hat{D}_{1-2}(\theta)$ is a displacement-like operator defined as

$$\hat{D}_{1-2}(\theta) = e^{\theta(\hat{a}_1\hat{a}_2^\dagger - \hat{a}_1^\dagger\hat{a}_2)} = e^{\tan(\theta)\hat{a}_1\hat{a}_2^\dagger} e^{\ln(\cos(\theta))(\hat{a}_1^\dagger\hat{a}_1 - \hat{a}_2^\dagger\hat{a}_2)} e^{-\tan(\theta)\hat{a}_1^\dagger\hat{a}_2}, \tag{13}$$

where θ is a real parameter, and the Wei–Norman theorem [39] has been employed to express the operator in factored form. The transformation defined through the operator in Equation (13) and its action on the field annihilation operators in Equations (A3) and (A4) formally resembles the standard beam–splitter transformation that mixes two field modes through an SU(2) unitary operation, a formalism that can be conveniently expressed in terms of angular–momentum operators [40]. We find that the Schrödinger equation in the new frame can be written as

$$i\frac{d|\varphi(t)\rangle}{dt} = \hat{D}_{1-2}(\theta)\hat{H}\hat{D}_{1-2}^\dagger(\theta)|\varphi(t)\rangle = \hat{H}_D|\varphi(t)\rangle, \tag{14}$$

and consequently, the evolution operator takes the form

$$U_D(t) = \hat{D}_{1-2}(\theta)\hat{U}(t)\hat{D}_{1-2}^\dagger(\theta), \tag{15}$$

where $\hat{U}(t)$ is given by Equation (10) with $N = 2$. Therefore, the Hamiltonian in the new frame, derived in Appendix B.1, can be written as

$$\begin{aligned}\hat{H}_D = \; & \omega_F \hat{I}_1 + g\hat{\sigma}_+(\hat{a}_1(\cos(\theta) - \sin(\theta)) + \hat{a}_2(\cos(\theta) + \sin(\theta))) \\ & + g\hat{\sigma}_-\left(\hat{a}_1^\dagger(\cos(\theta) - \sin(\theta)) + \hat{a}_2^\dagger(\cos(\theta) + \sin(\theta))\right).\end{aligned} \tag{16}$$

By choosing an appropriate value of θ, we can eliminate the operators associated with one of the fields. Specifically, setting $\theta = -\frac{\pi}{4}$ eliminates field 2, whereas $\theta = \frac{\pi}{4}$ eliminates field 1. For $\theta = -\frac{\pi}{4}$, the Hamiltonian becomes

$$\hat{H}_D = \omega_F \hat{I}_1 + \sqrt{2}g\left(\hat{\sigma}_+\hat{a}_1 + \hat{\sigma}_-\hat{a}_1^\dagger\right), \tag{17}$$

which can be identified as the Jaynes–Cummings Hamiltonian with an effective coupling constant $\tilde{g} = \sqrt{2}g$, larger than the individual atom–field coupling, plus the free Hamiltonian of a quantized field. A similar transformation procedure was reported in Ref. [35], where the interaction of a two–level atom with two field modes of different coupling strengths was considered. In contrast, in the present work the couplings are assumed to be identical, a condition required for the invariants previously defined to remain constant in time. Since the Jaynes–Cummings model is well known [3–5], its corresponding evolution operator can be readily written. The evolution of the state in this new frame is given by

$$|\varphi(t)\rangle = \hat{U}_D(t)|\varphi(0)\rangle = e^{-i\hat{H}_D t}|\varphi(0)\rangle, \tag{18}$$

where

$$\begin{aligned}\hat{U}_D(t) =& e^{-i\omega_F \hat{I}_1 t} e^{-i\tan\left(gt\sqrt{\hat{I}_{2D}+1}\right)\hat{A}_{2D}^\dagger} e^{\ln\left[\cos\left(gt\sqrt{\hat{I}_{2D}+1}\right)\right]\hat{\sigma}_z} e^{-i\tan\left(gt\sqrt{\hat{I}_{2D}+1}\right)\hat{A}_{2D}} \\ =& e^{-i\omega_F \hat{I}_1 t}\begin{bmatrix} \cos\left(\tilde{g}t\sqrt{\hat{n}_1+1}\right) & -i\frac{\sin\left(\tilde{g}t\sqrt{\hat{n}_1+1}\right)}{\sqrt{\hat{n}_1+1}}\hat{a}_1 \\ -i\hat{a}_1^\dagger\frac{\sin\left(\tilde{g}t\sqrt{\hat{n}_1+1}\right)}{\sqrt{\hat{n}_1+1}} & \cos\left(\tilde{g}t\sqrt{\hat{n}_1}\right)\end{bmatrix},\end{aligned} \tag{19}$$

with $\hat{n}_1 = \hat{a}_1^\dagger\hat{a}_1$, where $\hat{I}_{2D} = \hat{D}_{1-2}(\theta)\hat{I}_2\hat{D}_{1-2}^\dagger(\theta)$, $\hat{A}_{2D} = \hat{D}_{1-2}(\theta)\hat{A}_2\hat{D}_{1-2}^\dagger(\theta)$, and $\hat{A}_{2D}^\dagger = \hat{D}_{1-2}(\theta)\hat{A}_2^\dagger\hat{D}_{1-2}^\dagger(\theta)$ are defined in Appendix B.1. To obtain this matrix expression, the exponential operators were expanded in a power series, expressing the Pauli operators in their matrix form in the atomic basis, and after performing the corresponding simplifications, the final result was obtained. Transforming back to the original frame, the evolution of the system is given by

$$|\psi(t)\rangle = \hat{D}_{1-2}^\dagger(\theta)\hat{U}_D(t)\hat{D}_{1-2}(\theta)|\psi(0)\rangle, \tag{20}$$

with $\theta = -\frac{\pi}{4}$.

Atomic Inversion and Average Photon Number

The system is assumed to be initially prepared in the state

$$|\psi(0)\rangle = C[c_1|\alpha_1\rangle|\alpha_2\rangle|e\rangle + c_2|\beta_1\rangle|\beta_2\rangle|g\rangle] = C\begin{bmatrix} c_1|\alpha_1\rangle|\alpha_2\rangle \\ c_2|\beta_1\rangle|\beta_2\rangle\end{bmatrix}, \tag{21}$$

where $C = \frac{1}{\sqrt{|c_1|^2+|c_2|^2}}$ is the normalization constant, c_1 and c_2 are complex coefficients, and $|\alpha_i\rangle$ and $|\beta_i\rangle$ denote coherent states of the fields entangled with the atomic excited state $|e\rangle$ and the ground state $|g\rangle$, respectively. The index $i = 1, 2$ labels the two fields under consideration.

A quantity of particular interest in the study of atom–field interactions is the atomic inversion, which characterizes the population difference between the excited and ground

states of the atom. It reflects the exchange of energy between the atom and the quantized fields and is obtained from the expectation value of the operator $\hat{\sigma}_z$, namely

$$\langle\psi(t)|\hat{\sigma}_z|\psi(t)\rangle = \langle\psi(0)|\hat{D}^{\dagger}_{1-2}(\theta)\hat{U}^{\dagger}_{D}(t)\hat{\sigma}_z\hat{U}_D(t)\hat{D}_{1-2}(\theta)|\psi(0)\rangle. \tag{22}$$

To evaluate this quantity, we first apply the operator $\hat{D}_{1-2}(\theta)$ to the initial state, obtaining

$$\hat{D}_{1-2}(\theta)|\psi(0)\rangle = C\begin{bmatrix} c_1|\alpha'\rangle|\alpha''\rangle \\ c_2|\beta'\rangle|\beta''\rangle \end{bmatrix} = C\begin{bmatrix} c_1 e^{-\frac{|\alpha'|^2}{2}}\sum_{k=0}^{\infty}\frac{\alpha'^k}{\sqrt{k!}}|k\rangle|\alpha''\rangle \\ c_2 e^{-\frac{|\beta'|^2}{2}}\sum_{l=0}^{\infty}\frac{\beta'^l}{\sqrt{l!}}|l\rangle|\beta''\rangle \end{bmatrix}, \tag{23}$$

where $|\alpha'\rangle$, $|\alpha''\rangle$, $|\beta'\rangle$ and $|\beta''\rangle$ are coherent states with amplitudes

$$\begin{aligned} \alpha' &= \alpha_1\cos(\theta) - \alpha_2\sin(\theta), \qquad \alpha'' = \alpha_1\sin(\theta) + \alpha_2\cos(\theta), \\ \beta' &= \beta_1\cos(\theta) - \beta_2\sin(\theta), \qquad \beta'' = \beta_1\sin(\theta) + \beta_2\cos(\theta), \end{aligned} \tag{24}$$

and $|k\rangle$, $|l\rangle$ are Fock states. By applying the evolution operator $\hat{U}_D(t)$ we obtain

$$\begin{aligned} &\hat{U}_D(t)\hat{D}_{1-2}(\theta)|\psi(0)\rangle = Ce^{-i\omega_F\hat{I}_1 t} \\ &\times\begin{bmatrix} c_1 e^{-\frac{|\alpha'|^2}{2}}\sum_{k=0}^{\infty}\frac{\alpha'^k}{\sqrt{k!}}\cos(\tilde{g}t\sqrt{k+1})|k\rangle|\alpha''\rangle - ic_2 e^{-\frac{|\beta'|^2}{2}}\sum_{l=0}^{\infty}\frac{\beta'^l}{\sqrt{l!}}\sin(\tilde{g}t\sqrt{l})|l-1\rangle|\beta''\rangle \\ -ic_1 e^{-\frac{|\alpha'|^2}{2}}\sum_{k=0}^{\infty}\frac{\alpha'^k}{\sqrt{k!}}\sin(\tilde{g}t\sqrt{k+1})|k+1\rangle|\alpha''\rangle + c_2 e^{-\frac{|\beta'|^2}{2}}\sum_{l=0}^{\infty}\frac{\beta'^l}{\sqrt{l!}}\cos(\tilde{g}t\sqrt{l})|l\rangle|\beta''\rangle \end{bmatrix}. \end{aligned} \tag{25}$$

Finally, by applying the operator $\hat{\sigma}_z$ to the result in Equation (25) and performing the necessary calculations, we obtain

$$\begin{aligned} &\langle\psi(t)|\hat{\sigma}_z|\psi(t)\rangle = \\ &C^2\Bigg[|c_1|^2 e^{-|\alpha'|^2}\sum_{k=0}^{\infty}\frac{|\alpha'|^{2k}}{k!}\cos(2\tilde{g}t\sqrt{k+1}) - |c_2|^2 e^{-|\beta'|^2}\sum_{k=0}^{\infty}\frac{|\beta'|^{2k}}{k!}\cos(2\tilde{g}t\sqrt{k}) \\ &+2e^{-\frac{|\alpha'|^2+|\beta'|^2}{2}}e^{-\frac{|\alpha''|^2+|\beta''|^2}{2}}\,\mathrm{Re}\Bigg\{ic_1c_2^{*}e^{\alpha''\beta''^{*}}\sum_{k=0}^{\infty}\frac{(\alpha'\beta'^{*})^k}{k!}\frac{\beta'^{*}}{\sqrt{k+1}}\sin(2\tilde{g}t\sqrt{k+1})\Bigg\}\Bigg]. \end{aligned} \tag{26}$$

It is worth emphasizing that, for a single field interacting with a two–level atom, the Rabi frequency depends on the atom–field coupling constant [5,41]. When two fields are present, this frequency increases and depends on the effective coupling $\tilde{g} = \sqrt{2}g$, reflecting the collective enhancement of the interaction strength. In Figure 2, the atomic inversion as a function of the dimensionless parameter $\omega_F t$ is shown for the case $c_1 = c_2 = \frac{1}{\sqrt{2}}$ and coupling constant $g = 0.1\omega_F$, with the fields initially prepared in coherent states. The solid colored lines represent the analytical results obtained from Equation (26), while the dashed curves correspond to the numerical solutions of the Schrödinger equation for the Hamiltonian in Equation (11). The analytical expressions involve infinite series that were truncated at $k_{\max} = 40$, although convergence tests showed that $k_{\max} = 30$ was sufficient, as larger values changed the observables by less than 10^{-8}. This criterion applies both to the atomic inversion and to the subsequent calculation of the mean photon number. The numerical simulations were carried out using the QuTiP library in Python 3.13.7 [42], specifically employing the `mesolve` function, with the Hilbert space of each field mode appropriately truncated. Convergence tests showed that a Hilbert–space dimension of 20 per mode was sufficient, since increasing it to 21 changed the observables by less than 10^{-7}. The same criterion was later applied to the calculation of the mean photon number, confirming that this Hilbert–space size is adequate, as further enlargement produces only negligible variations compared to the magnitude of the observables and within the desired

numerical precision. As an additional consistency check of the Hilbert–space truncation, the expectation value of the commutator $[\hat{a}(t), \hat{a}^{\dagger}(t)]$ was computed for each of the field modes involved using QuTiP, and it remained close to unity in all cases, confirming that the chosen Fock basis was sufficiently large for accurate results. In the case $\alpha_1 = \alpha_2 = \beta_1 = \beta_2 = 0$, where both fields are initially prepared in the vacuum state, Rabi oscillations appear, revealing the periodic exchange of excitations between the atom and the quantized fields. In contrast, for $\alpha_1 = 0$, $\alpha_2 = 1$, $\beta_1 = 0$, $\beta_2 = 1$, and for $\alpha_1 = 1$, $\alpha_2 = 0$, $\beta_1 = 1$, $\beta_2 = 0$, the dynamics become more elaborate; however, as expected, both initial conditions lead to the same dynamical behavior. Finally, for $\alpha_1 = \alpha_2 = 2$ and $\beta_1 = \beta_2 = 0$, the atomic inversion exhibits the well–known collapse and revival phenomenon, arising from the quantized nature of the two field modes and their collective coupling to the atom. The predominantly negative values of the atomic inversion arise from the specific choice of initial parameters. However, this behavior is not general: increasing the coherent amplitudes or choosing complex values for c_1, c_2, or for the field amplitudes can lead to positive or more intricate inversion dynamics.

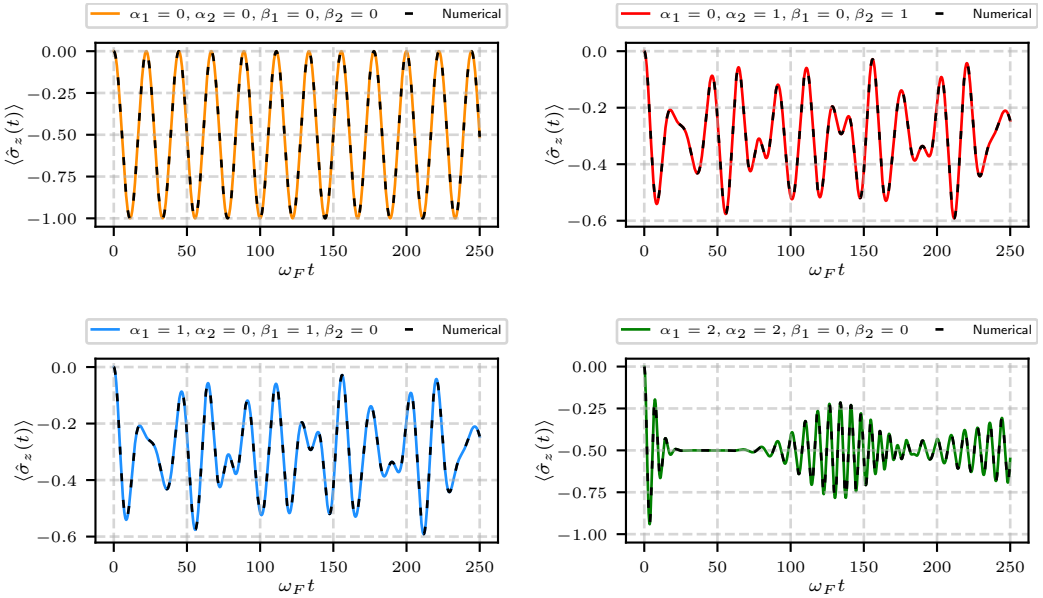


Figure 2. Atomic inversion as a function of the dimensionless parameter $\omega_F t$ for various amplitudes of the initial coherent field states. The parameters used are $c_1 = c_2 = \frac{1}{\sqrt{2}}$ and $g = 0.1\omega_F$. Solid colored lines denote the analytical results, while dashed curves correspond to the numerical simulations obtained using QuTiP [42].

Following the same procedure, we compute the time evolution of the average photon number in field 1, which is given by

$$\langle \psi(t)|\hat{a}_1^{\dagger}\hat{a}_1|\psi(t)\rangle = \langle \psi(0)|\hat{D}_{1-2}^{\dagger}(\theta)\hat{U}_D^{\dagger}(t)\hat{D}_{1-2}(\theta)\hat{a}_1^{\dagger}\hat{a}_1\hat{D}_{1-2}^{\dagger}(\theta)\hat{U}_D(t)\hat{D}_{1-2}(\theta)|\psi(0)\rangle, \quad (27)$$

where the photon number operator $\hat{a}_1^{\dagger}\hat{a}_1$ corresponding to field 1 transforms under the action of $\hat{D}_{1-2}(\theta)$ as

$$\hat{D}_{1-2}(\theta)\hat{a}_1^{\dagger}\hat{a}_1\hat{D}_{1-2}^{\dagger}(\theta) = \hat{a}_1^{\dagger}\hat{a}_1\cos^2(\theta) + \hat{a}_2^{\dagger}\hat{a}_2\sin^2(\theta) + (\hat{a}_1^{\dagger}\hat{a}_2 + \hat{a}_1\hat{a}_2^{\dagger})\cos(\theta)\sin(\theta). \quad (28)$$

Thus, the average photon number in field 1 is given by

$$
\begin{aligned}
&\langle\psi(t)|\hat{a}_1^\dagger\hat{a}_1|\psi(t)\rangle = \\
&C^2\Bigg[|c_1|^2\Big(|\alpha'|^2\cos^2(\theta)+|\alpha''|^2\sin^2(\theta)\Big)+|c_1|^2e^{-|\alpha'|^2}\sum_{k=0}^{\infty}\frac{|\alpha'|^{2k}}{k!}\Big[\cos^2(\theta)\,S_{k+1}^2 \\
&+\sin(2\theta)\Big(C_{k+1}C_{k+2}+\frac{\sqrt{k+2}}{\sqrt{k+1}}S_{k+1}S_{k+2}\Big)\,\mathrm{Re}\{\alpha'^*\alpha''\}\Big] \\
&+|c_2|^2\Big(|\beta'|^2\cos^2(\theta)+|\beta''|^2\sin^2(\theta)\Big)+|c_2|^2e^{-|\beta'|^2}\sum_{k=0}^{\infty}\frac{|\beta'|^{2k}}{k!}\Big[-\cos^2(\theta)\,S_k^2 \\
&+\sin(2\theta)\Big(C_kC_{k+1}+\frac{\sqrt{k}}{\sqrt{k+1}}S_kS_{k+1}\Big)\,\mathrm{Re}\{\beta'^*\beta''\}\Big] \\
&-e^{-\frac{|\alpha'|^2+|\beta'|^2}{2}}e^{-\frac{|\alpha''|^2+|\beta''|^2}{2}}\,\mathrm{Re}\Bigg\{ic_1c_2^*e^{\alpha''\beta''^*}\sum_{k=0}^{\infty}\frac{(\alpha'\beta'^*)^k}{k!}\Bigg[\frac{\beta'^*}{\sqrt{k+1}}\sin(2\tilde{g}t\sqrt{k+1})\cos^2(\theta) \\
&+\sin(2\theta)\Big[\beta''^*\big(\sqrt{k+1}C_kS_{k+1}-\sqrt{k}C_{k+1}S_k\big) \\
&+\alpha''\beta'^{*2}\Big(\frac{1}{\sqrt{k+1}}C_{k+2}S_{k+1}-\frac{1}{\sqrt{k+2}}C_{k+1}S_{k+2}\Big)\Big]\Bigg]\Bigg\}\Bigg],
\end{aligned}
\tag{29}
$$

where we have defined the auxiliary functions $C_k = \cos(\tilde{g}t\sqrt{k})$ and $S_k = \sin(\tilde{g}t\sqrt{k})$. In Figure 3, we show the time evolution of the mean photon number in field 1 for the same parameters as in Figure 2. The solid lines correspond to the analytical results from Equation (29), while the dashed curves represent the numerical solutions of the Schrödinger equation. For vacuum initial states ($\alpha_1 = \alpha_2 = \beta_1 = \beta_2 = 0$), Rabi–type oscillations appear, reflecting the exchange of excitations between the atom and the fields. For larger coherent amplitudes, the dynamics become more intricate and exhibit oscillations characteristic of collapse and revival phenomena, in agreement with the behavior of the atomic inversion. It is worth noting that the initial mean photon number in field 1 results from the weighted contributions of both components of the entangled atom–field state given in Equation (21), namely, $\langle\hat{a}_1^\dagger\hat{a}_1(0)\rangle = |C|^2\big(|c_1|^2|\alpha_1|^2+|c_2|^2|\beta_1|^2\big)$.

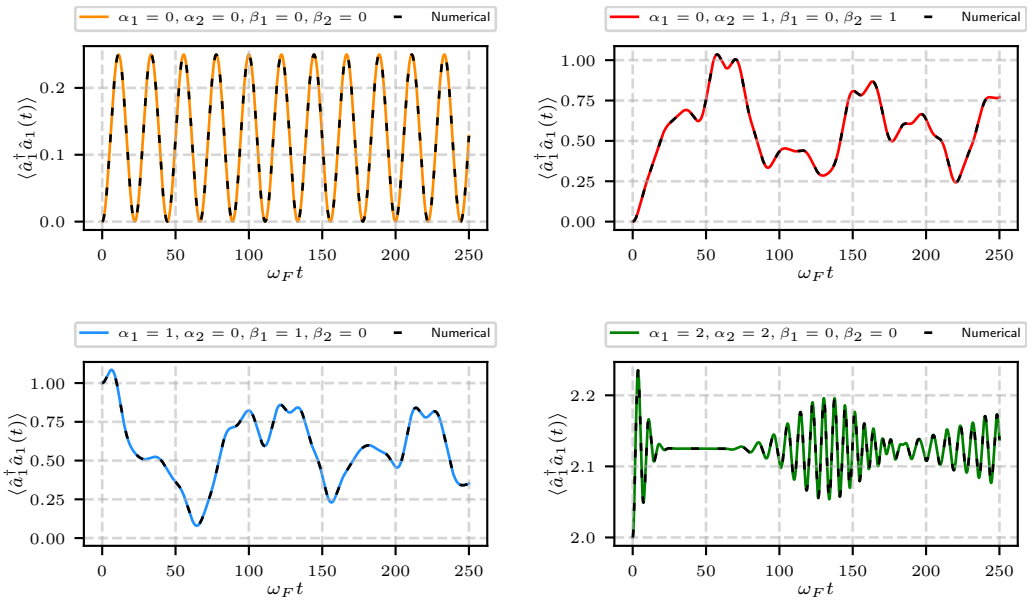


Figure 3. Mean photon number in field 1 as a function of the dimensionless parameter $\omega_F t$ for various amplitudes of the initial coherent field states. The parameters used are $c_1 = c_2 = \frac{1}{\sqrt{2}}$ and $g = 0.1\omega_F$. Solid colored lines denote the analytical results, while dashed curves correspond to the numerical simulations.

4. Three Quantized Fields Interacting with the Atom

We now consider the case of three quantized fields interacting with a two–level atom. The Hamiltonian describing this system is given by

$$\hat{H} = \omega_F \hat{I}_1 + g\sqrt{\hat{I}_2 + \frac{3}{2}}\left(\hat{A}_3 + \hat{A}_3^\dagger\right), \tag{30}$$

where the invariants given in Equations (4) and (5) are evaluated for $N = 3$. Similarly to the $N = 2$ case, we apply a unitary transformation to move to a new reference frame where all field operators, except those associated with field 1, are eliminated. In this transformed frame, the Schrödinger equation can be solved more straightforwardly. The transformation is defined as

$$\hat{D}_{1-3}(\theta) = e^{\theta\left(\hat{a}_1 \hat{B}_{2-3}^\dagger - \hat{a}_1^\dagger \hat{B}_{2-3}\right)}, \tag{31}$$

where

$$\hat{B}_{2-3} = \frac{\hat{a}_2 + \hat{a}_3}{\sqrt{2}}. \tag{32}$$

Therefore, the Hamiltonian in the transformed frame takes the form (see Appendix B.2)

$$\begin{aligned}\hat{H}_D = \omega_F \hat{I}_1 &+ g\sigma_+\left[\hat{a}_1\left(\cos(\theta) - \sqrt{2}\sin(\theta)\right) + \hat{B}_{2-3}\left(\sin(\theta) + \sqrt{2}\cos(\theta)\right)\right] \\ &+ g\sigma_-\left[\hat{a}_1^\dagger\left(\cos(\theta) - \sqrt{2}\sin(\theta)\right) + \hat{B}_{2-3}^\dagger\left(\sin(\theta) + \sqrt{2}\cos(\theta)\right)\right].\end{aligned} \tag{33}$$

By setting $\theta = \arctan(-\sqrt{2})$, the interaction terms involving fields 2 and 3 vanish, and the Hamiltonian reduces to

$$\hat{H}_D = \omega_F \hat{I}_1 + g\left(\cos(\theta) - \sqrt{2}\sin(\theta)\right)\sigma_+ \hat{a}_1 + g\left(\cos(\theta) - \sqrt{2}\sin(\theta)\right)\sigma_- \hat{a}_1^\dagger. \tag{34}$$

Through this transformation, we obtain an effective Jaynes–Cummings Hamiltonian for a single field, characterized by an effective coupling constant $\tilde{g} = \left(\cos\theta - \sqrt{2}\sin\theta\right)g \approx 1.732g$, together with the free–field Hamiltonian of the remaining quantized modes (2 and 3). Since the evolution operator $\hat{U}_D(t)$ associated with this Hamiltonian is already known, the evolution of the system in the original frame can be expressed as

$$|\psi(t)\rangle = \hat{D}_{1-3}^\dagger(\theta)\hat{U}_D(t)\hat{D}_{1-3}(\theta)|\psi(0)\rangle, \tag{35}$$

with $\theta = \arctan(-\sqrt{2})$.

Atomic Inversion and Average Number of Photons

We assume that the system is initially prepared in the state

$$|\psi(0)\rangle = C[c_1|\alpha_1\rangle|\alpha_2\rangle|\alpha_3\rangle|e\rangle + c_2|\beta_1\rangle|\beta_2\rangle|\beta_3\rangle|g\rangle] = C\begin{bmatrix} c_1|\alpha_1\rangle|\alpha_2\rangle|\alpha_3\rangle \\ c_2|\beta_1\rangle|\beta_2\rangle|\beta_2\rangle \end{bmatrix}. \tag{36}$$

To determine the system's evolution, we first apply the operator $\hat{D}_{1-3}(\theta)$ to the initial state. Before doing so, however, it is convenient to express this operator in factored form. This procedure follows directly by analogy with the $N = 2$ case, Equation(13), since the operators involved satisfy the same commutation relations. In particular, because $\hat{B}_{2-3}$ obeys the relation $\left[\hat{B}_{2-3}, \hat{B}_{2-3}^\dagger\right] = 1$, the same method can be applied here, yielding

$$\hat{D}_{1-3}(\theta) = e^{\theta\left(\hat{a}_1 \hat{B}_{2-3}^\dagger - \hat{a}_1^\dagger \hat{B}_{2-3}\right)} = e^{\tan(\theta)\hat{a}_1 \hat{B}_{2-3}^\dagger} e^{\ln(\cos(\theta))\left(\hat{a}_1^\dagger \hat{a}_1 - \hat{B}_{2-3}^\dagger \hat{B}_{2-3}\right)} e^{-\tan(\theta)\hat{a}_1^\dagger \hat{B}_{2-3}}, \tag{37}$$

where

$$e^{\ln(\cos(\theta))(\hat{a}_1^\dagger\hat{a}_1-\hat{B}_{2-3}^\dagger\hat{B}_{2-3})}=e^{\ln(\cos(\theta))(\hat{a}_1^\dagger\hat{a}_1-\frac{1}{2}(\hat{a}_2^\dagger\hat{a}_2+\hat{a}_3^\dagger\hat{a}_3))}e^{-\frac{\ln(\cos(\theta))}{2}(\hat{a}_2\hat{a}_3^\dagger+\hat{a}_2^\dagger\hat{a}_3)}. \tag{38}$$

The last exponential in this expression can be factorized analogously to Equation (37), since the involved operators form a closed algebra under the commutator. Hence, the Wei–Norman theorem [39] can be applied, yielding

$$e^{\chi(\hat{a}_2\hat{a}_3^\dagger+\hat{a}_2^\dagger\hat{a}_3)}=e^{F\hat{a}_2\hat{a}_3^\dagger}e^{G(\hat{a}_2^\dagger\hat{a}_2-\hat{a}_3^\dagger\hat{a}_3)}e^{F\hat{a}_2^\dagger\hat{a}_3}, \tag{39}$$

where $\chi=-\frac{\ln(\cos(\theta))}{2}$, and

$$F=\tanh(\chi),\qquad G=-\ln(1-\tanh(\chi))-\chi. \tag{40}$$

Once the operator $\hat{D}_{1-3}(\theta)$ has been factorized, and after performing the necessary algebraic manipulations while taking into account that

$$\hat{D}_{1-3}(\theta)\hat{a}_1^\dagger\hat{a}_1\hat{D}_{1-3}^\dagger(\theta)=\left(\hat{a}_1^\dagger\cos(\theta)+\frac{\hat{a}_2^\dagger+\hat{a}_3^\dagger}{\sqrt{2}}\sin(\theta)\right)\left(\hat{a}_1\cos(\theta)+\frac{\hat{a}_2+\hat{a}_3}{\sqrt{2}}\sin(\theta)\right), \tag{41}$$

we obtain the atomic inversion

$$\begin{aligned}\langle\psi(t)|\hat{\sigma}_z|\psi(t)\rangle&=\langle\psi(0)|\hat{D}_{1-3}^\dagger(\theta)\hat{U}_D^\dagger(t)\hat{\sigma}_z\hat{U}_D(t)\hat{D}_{1-3}(\theta)|\psi(0)\rangle\\&=C^2\Bigg[|f_1|^2e^{-|\alpha'|^2}\sum_{k=0}^{\infty}\frac{|\alpha'|^{2k}}{k!}\cos(2\tilde{g}t\sqrt{k+1})-|f_2|^2e^{-|\beta'|^2}\sum_{k=0}^{\infty}\frac{|\beta'|^{2k}}{k!}\cos(2\tilde{g}t\sqrt{k})\\&\quad+2e^{-\frac{1}{2}(|\alpha'|^2+|\alpha''|^2+|\alpha'''|^2+|\beta'|^2+|\beta''|^2+|\beta''|^2)}\\&\quad\times\mathrm{Re}\left\{if_1f_2^*e^{\alpha''\beta''^*+\alpha'''\beta'''^*}\sum_{k=0}^{\infty}\frac{(\alpha'\beta'^*)^k}{k!}\frac{\beta'^*}{\sqrt{k+1}}\sin(2\tilde{g}t\sqrt{k+1})\right\}\Bigg],\end{aligned} \tag{42}$$

and the average number of photons

$$\begin{aligned}&\langle\psi(t)|\hat{a}_1^\dagger\hat{a}_1|\psi(t)\rangle=\\&C^2\Bigg[|f_1|^2\left(|\alpha'|^2\cos^2(\theta)+\frac{1}{2}|\alpha''+\alpha'''|^2\sin^2(\theta)\right)+|f_1|^2e^{-|\alpha'|^2}\sum_{k=0}^{\infty}\frac{|\alpha'|^{2k}}{k!}\Big[\cos^2(\theta)S_{k+1}^2\\&+\frac{1}{\sqrt{2}}\sin(2\theta)\,\mathrm{Re}\{\alpha'^*(\alpha''+\alpha''')\}\left(C_{k+1}C_{k+2}+\frac{\sqrt{k+2}}{\sqrt{k+1}}S_{k+1}S_{k+2}\right)\Big]\\&+|f_2|^2\left(|\beta'|^2\cos^2(\theta)+\frac{1}{2}|\beta''+\beta'''|^2\sin^2(\theta)\right)+|f_2|^2e^{-|\beta'|^2}\sum_{k=0}^{\infty}\frac{|\beta'|^{2k}}{k!}\Big[-\cos^2(\theta)S_k^2\\&+\frac{1}{\sqrt{2}}\sin(2\theta)\,\mathrm{Re}\{\beta'^*(\beta''+\beta''')\}\left(C_kC_{k+1}+\frac{\sqrt{k}}{\sqrt{k+1}}S_kS_{k+1}\right)\Big]\\&-e^{-\frac{1}{2}(|\alpha'|^2+|\alpha''|^2+|\alpha'''|^2+|\beta'|^2+|\beta''|^2+|\beta'''|^2)}\\&\times\mathrm{Re}\Bigg\{if_1f_2^*e^{\alpha''\beta''^*}e^{\alpha'''\beta'''^*}\sum_{k=0}^{\infty}\frac{(\alpha'\beta'^*)^k}{k!}\Bigg[\frac{\beta'^*}{\sqrt{k+1}}\sin(2\tilde{g}t\sqrt{k+1})\cos^2(\theta)\\&+\frac{\sin(2\theta)}{\sqrt{2}}\Big[(\beta''^*+\beta'''^*)(\sqrt{k+1}C_kS_{k+1}-\sqrt{k}C_{k+1}S_k)\\&+(\alpha''+\alpha''')\beta'^{*2}\left(\frac{1}{\sqrt{k+1}}C_{k+2}S_{k+1}-\frac{1}{\sqrt{k+2}}C_{k+1}S_{k+2}\right)\Big]\Bigg]\Bigg\}\Bigg],\end{aligned} \tag{43}$$

where C_k and S_k have the same form as in the two–field case, but with the effective coupling constant $\tilde{g}$ specific to this configuration and

$$f_1 = c_1 e^{-\frac{1}{2}(|\alpha_1|^2+|\alpha_2|^2+|\alpha_3|^2)} e^{\frac{1}{2}(|\alpha'|^2+|\alpha''|^2+|\alpha'''|^2)}, \tag{44}$$

$$f_2 = c_2 e^{-\frac{1}{2}(|\beta_1|^2+|\beta_2|^2+|\beta_3|^2)} e^{\frac{1}{2}(|\beta'|^2+|\beta''|^2+|\beta'''|^2)}, \tag{45}$$

$$\begin{aligned} \gamma' &= (\gamma_1+\gamma_2+\gamma_3)e^{-2\chi}, \\ \gamma'' &= (F\gamma_3+\gamma_2)e^{\chi+G}-\gamma', \\ \gamma''' &= F(F\gamma_3+\gamma_2)e^{\chi+G}-\gamma'+\gamma_3 e^{\chi-G}, \end{aligned} \tag{46}$$

with $\gamma = \alpha, \beta$. As observed, when three quantized fields interact with the atom, the Rabi frequency depends on the effective coupling constant $\tilde{g}$, which is larger than the individual atom–field coupling and also greater than that obtained in the two–field case. This enhancement results from the collective action of multiple fields coupling to the same atomic transition. Hence, increasing the number of fields is expected to further enhance the effective coupling and the corresponding oscillation frequency, leading to faster Rabi oscillations. In Figures 4 and 5, we present the atomic inversion and the average photon number, respectively, as a function of the dimensionless parameter $\omega_F t$. The amplitudes of fields 1 and 2 are chosen to be the same as in the $N = 2$ case, while field 3 is initially prepared in the vacuum state. This configuration enables a direct comparison of the system's dynamics for $N = 2$ and $N = 3$, allowing us to identify the specific influence of the additional quantized mode on the atom–field interaction. In this case, the analytical series were truncated at $k_{\max} = 40$, since convergence tests performed with $k_{\max} = 30$ showed that further increases changed the observables by less than 10^{-13}. The numerical simulations, carried out with the QuTiP library in Python, used Hilbert spaces of dimension 25 per mode, which proved sufficient since enlarging them to 26 produced variations smaller than 10^{-6}.

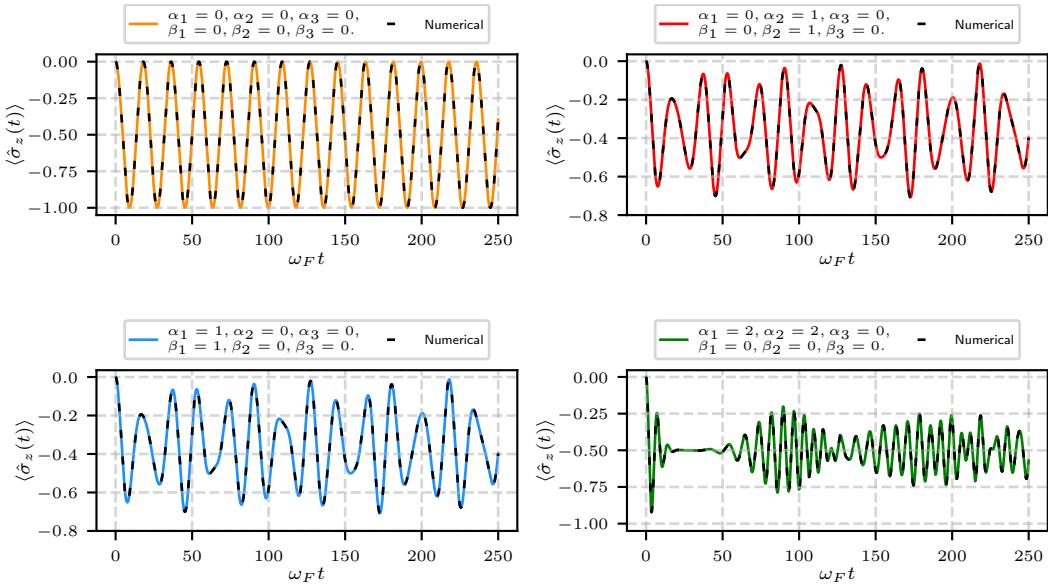


Figure 4. Atomic inversion as a function of the dimensionless parameter $\omega_F t$ for the case of three quantized fields interacting with a two-level atom, for various amplitudes of the initial coherent field states. The parameters used are $c_1 = c_2 = \frac{1}{\sqrt{2}}$ and $g = 0.1\omega_F$. Solid colored lines denote the analytical results, and dashed curves correspond to the numerical simulations.

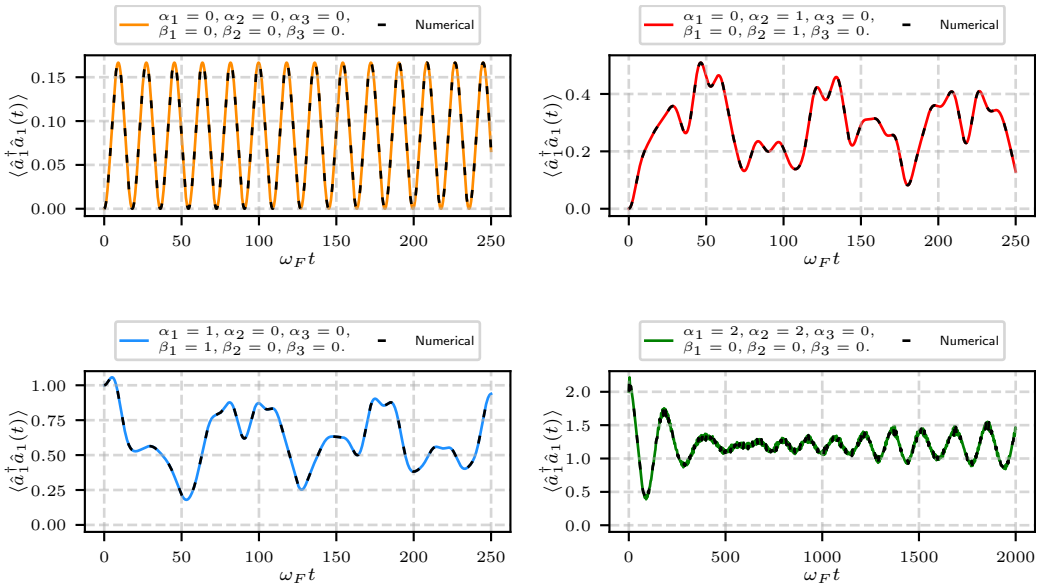


Figure 5. Average photon number in field 1 as a function of the dimensionless parameter $\omega_F t$ for the case of three quantized fields interacting with a two-level atom, for various amplitudes of the initial coherent field states. The parameters used are $c_1 = c_2 = \frac{1}{\sqrt{2}}$ and $g = 0.1\omega_F$. Solid colored lines denote the analytical results, and dashed curves correspond to the numerical simulations.

As we can see, the dynamics of the atomic inversion resemble those observed in the case where two fields interact with the atom. We observe Rabi oscillations with a higher frequency, as well as collapses and revivals that occur more rapidly than in the case $N = 2$. This behavior indicates that the presence of a third field, even when initially in the vacuum state, modifies the effective coupling between the atom and the radiation modes, leading to a faster exchange of energy between the atomic and field subsystems. In the framework of the Jaynes–Cummings model, it is well known that the revival time of the atomic inversion [6], τ_{rev}, depends inversely on the atom–field coupling constant and on the square root of the average photon number. Specifically, it is given by

$$\tau_{\text{rev}} = \frac{2\pi}{g}|\alpha|, \tag{47}$$

where g denotes the atom-field coupling constant. This relation, valid in the regime of large coherent-state amplitudes and for long evolution times, shows that an increase in the coupling strength leads to a shorter revival time–consistent with the faster revivals observed when three fields interact with the atom. On the other hand, for the average photon number we observe a similar dynamics to that found in the case $N = 2$. The main difference is that, in the subplot where the collapse and revival phenomena were clearly observed for the $N = 2$ case, such behavior becomes much less pronounced when the third field is included. Although a gradual decrease in the oscillations can still be seen—reminiscent of the collapse dynamics—the subsequent rephasing that characterizes the revivals is no longer clearly distinguishable. This suggests that the presence of a third field, even when initially in the vacuum state, alters the redistribution of excitations among the modes, thereby modifying the conditions under which rephasing can occur.

5. Generalization to N Fields

Following the same reasoning employed in the cases $N = 2$ and $N = 3$, we now outline the procedure used to generalize these specific scenarios to the case of N quan-

tized fields interacting with a two–level atom. To this end, we apply the corresponding generalized transformation

$$\hat{D}_{1-N}(\theta) = e^{\theta\left(\hat{a}_1 \hat{B}_{2-N}^{\dagger} - \hat{a}_1^{\dagger} \hat{B}_{2-N}\right)}, \tag{48}$$

where

$$\hat{B}_{2-N} = \frac{\sum_{k=2}^{N} \hat{a}_k}{\sqrt{N-1}}. \tag{49}$$

The reason for defining $\hat{D}_{1-N}(\theta)$ in this manner is that the operator $\hat{B}_{2-N}$ satisfies the commutation relation $\left[\hat{B}_{2-N}, \hat{B}_{2-N}^{\dagger}\right] = 1$, which allows us to write

$$\hat{D}_{1-N}(\theta) = e^{\theta\left(\hat{a}_1 \hat{B}_{2-N}^{\dagger} - \hat{a}_1^{\dagger} \hat{B}_{2-N}\right)} = e^{\tan(\theta)\hat{a}_1 \hat{B}_{2-N}^{\dagger}} e^{\ln(\cos(\theta))(\hat{a}_1^{\dagger}\hat{a}_1 - \hat{B}_{2-N}^{\dagger}\hat{B}_{2-N})} e^{-\tan(\theta)\hat{a}_1^{\dagger}\hat{B}_{2-N}}, \tag{50}$$

and, together with the fact that the operators resulting from $\hat{B}_{2-N}^{\dagger}\hat{B}_{2-N}$ are products of the form $\hat{a}_j \hat{a}_k^{\dagger}$, where each $\hat{a}_k$ satisfies the same commutation relations, they therefore close an algebra under the commutation operation. This property allows us to decouple the exponential by means of the Wei–Norman theorem [39] and, consequently, to factorize the operator $\hat{D}_{1-N}(\theta)$ so that it can be consistently applied to the initial condition of the system. The Hamiltonian of the system in the new reference frame is given by (see Appendix B.3)

$$\begin{aligned} \hat{H}_D = \omega_F \hat{I}_1 &+ g\sigma_+ \left[\hat{a}_1 \left(\cos(\theta) - \sqrt{N-1}\sin(\theta)\right) + \hat{B}_{2-N}\left(\sin(\theta) + \sqrt{N-1}\cos(\theta)\right)\right] \\ &+ g\sigma_- \left[\hat{a}_1^{\dagger}\left(\cos(\theta) - \sqrt{N-1}\sin(\theta)\right) + \hat{B}_{2-N}^{\dagger}\left(\sin(\theta) + \sqrt{N-1}\cos(\theta)\right)\right]. \end{aligned} \tag{51}$$

If we set

$$\theta = \tan^{-1}(-\sqrt{N-1}), \tag{52}$$

all fields except field 1 are eliminated, and in this way we obtain the Hamiltonian

$$\hat{H}_D = \omega_F \hat{I}_1 + g\left(\cos(\theta) - \sqrt{N-1}\sin(\theta)\right)\sigma_+ \hat{a}_1 + g\left(\cos(\theta) - \sqrt{N-1}\sin(\theta)\right)\sigma_- \hat{a}_1^{\dagger}, \tag{53}$$

which corresponds to a Jaynes–Cummings Hamiltonian with an effective coupling constant $\tilde{g} = g\left(\cos\theta - \sqrt{N-1}\sin\theta\right)$, plus the free Hamiltonian of the remaining $N-1$ fields. Since the evolution operator associated with this Hamiltonian is already known, the atomic inversion and the mean photon number can be readily obtained by applying the corresponding operators when the initial state is composed of coherent field states. The main challenge arises from the fact that, as N increases, the number of algebraic manipulations required grows significantly. Moreover, as the number of interacting field modes N increases, the parameter θ tends toward $-\frac{\pi}{2}$, leading to an effective coupling constant $\tilde{g} \to g\sqrt{N-1}$. This suggests that the atom–field interaction strength, and consequently the Rabi frequency, increase with N, reflecting a collective enhancement effect resulting from the simultaneous coupling of multiple quantized fields to the atom. It is worth noting that the dynamical invariants $\hat{I}_1$ and $\hat{I}_2$ provide a simplified geometric framework for the system. While developing a full phase–space representation for N fields is challenging due to its high dimensionality, the use of invariant quantities—a strategy that has proven useful for visualizing dynamics in other systems [43]—allows for a more manageable description. In our case, the transformation $\hat{D}_{1-N}(\theta)$ maps the multi-mode evolution onto a single–mode trajectory within a collective Bloch sphere. This algebraic reduction clarifies how the collective coupling governs the collapse–revival phenomena by effectively working within a simplified SU(2) subspace.

6. Conclusions

We have presented a general and unified procedure to describe the dynamics of N degenerate quantized fields resonantly interacting with a single two–level atom within the rotating–wave approximation. By identifying an appropriate set of dynamical invariants, the full evolution operator can be systematically factorized, allowing the multimode Hamiltonian to be mapped; through a suitable unitary transformation, onto an effective Jaynes–Cummings form. A central outcome of this construction is the emergence of an effective coupling constant $\tilde{g}$ that *increases monotonically with the number of interacting fields*. This scaling encapsulates a genuine collective enhancement: as additional degenerate modes participate coherently in the interaction, the atom experiences a progressively stronger effective coupling, reflected in an amplified Rabi frequency and a more pronounced dynamical response.

The explicit implementations for the cases of two and three quantized fields illustrate the structure and transparency of the general method. These examples reveal how the invariants, unitary reduction, and effective Hamiltonian emerge in a natural and hierarchical fashion, providing a clear pathway for extending the analysis to an arbitrary number N of degenerate modes. For initially coherent field states and an atom prepared in a superposition of its internal levels, we computed the atomic inversion and mean photon number, observing vacuum Rabi oscillations as well as the characteristic collapse–revival phenomenon. Overall, the procedure developed here not only generalizes the Jaynes–Cummings model to a multimode scenario while preserving its essential physical content, but also demonstrates how the collective increase in the effective coupling strength enriches the dynamical behavior. This framework provides a robust foundation for exploring more elaborate multimode quantum–optical configurations and for analyzing cooperative atom-field effects in increasingly complex quantum architectures.

Author Contributions: Conceptualization, M.A.G.-M. and I.R.-P.; Methodology, M.A.G.-M. and I.R.-P.; Investigation, M.A.G.-M., I.R.-P. and H.M.M.-C.; Writing—original draft, M.A.G.-M., I.R.-P. and H.M.M.-C.; Supervision, H.M.M.-C. All authors contributed equally to each of the requirements necessary for the elaboration of this manuscript. All authors have read and agreed to the published version of the manuscript.

Funding: This research received no external funding.

Data Availability Statement: No new data were created or analyzed in this study. The original contributions presented in this study are included in the article. Further inquiries can be directed to the corresponding author.

Acknowledgments: Marco Antonio García-Márquez thanks the Secretariat of Science, Humanities, Technology and Innovation (SECIHTI) and the National Institute of Astrophysics, Optics and Electronics (INAOE) for the doctoral scholarship.

Conflicts of Interest: The authors declare no conflict of interest.

Appendix A. Wei–Norman Theorem to Express the Temporal Evolution in a Factored Form

Since the operators involved in the last exponential of the evolution operator in Equation (9) form a closed algebra (see Equation (7)), and the evolution operator satisfies the Schrödinger equation $\frac{d\hat{U}}{dt} = -i\hat{H}\hat{U}$, we can apply the Wei–Norman theorem [39] to express that exponential in a factored form, yielding

$$\hat{U}(t) = e^{-i\omega_F \hat{I}_1 t} e^{f_1(t)\hat{A}_N^\dagger} e^{f_2(t)\hat{\sigma}_z} e^{f_3(t)\hat{A}_N}, \tag{A1}$$

where the functions $f_i(t)$ are to be determined and satisfy the condition $f_i(0) = 0$. Thus, taking the derivative of Equation (A1) and comparing it with $-i\hat{H}\hat{U}$, with $\hat{H}$ given by Equation (8) and assuming $\Delta = 0$, we obtain the following set of differential equations for the f_i functions:

$$\begin{aligned} 0 &= \dot{f}_2 - f_1 \dot{f}_3 e^{2f_2}, \\ -ig\sqrt{\hat{I}_2 + \frac{N}{2}} &= \dot{f}_3 e^{2f_2}, \\ -ig\sqrt{\hat{I}_2 + \frac{N}{2}} &= \dot{f}_1 + 2f_1\dot{f}_2 - f_1^2 \dot{f}_3 e^{2f_2}. \end{aligned} \tag{A2}$$

By solving these equations, we obtain the factorized form of the evolution operator, given by Equation (10).

Appendix B. Transformation of the Hamiltonian Under the Operator $\hat{D}_{1-N}$

In this appendix, we present the transformation of the relevant operators under the action of the operator $\hat{D}_{1-N}(\theta)$ for systems with two, three, and N quantized fields interacting with a two–level atom, leading to the corresponding transformed Hamiltonian in each case.

Appendix B.1. $N = 2$

We consider the case in which two quantized fields interact with a two–level atom. The annihilation operators corresponding to both fields transform under the action of $\hat{D}_{1-2}(\theta)$ as follows:

$$\hat{D}_{1-2}(\theta)\hat{a}_1\hat{D}^\dagger_{1-2}(\theta) = \hat{a}_1\cos(\theta) + \hat{a}_2\sin(\theta), \tag{A3}$$

$$\hat{D}_{1-2}(\theta)\hat{a}_2\hat{D}^\dagger_{1-2}(\theta) = \hat{a}_2\cos(\theta) - \hat{a}_1\sin(\theta). \tag{A4}$$

Using the results from Equations (A3) and (A4), we find that the operators appearing in the evolution operator, Equation (10), transform as follows: the excitation number operator $\hat{I}_1$ remains unchanged

$$\hat{I}_{1D} = \hat{D}_{1-2}(\theta)\hat{I}_1\hat{D}^\dagger_{1-2}(\theta) = \hat{I}_1, \tag{A5}$$

while the operators $\hat{I}_2$, $\hat{A}_2$, and $\hat{A}^\dagger_2$ transform as

$$\begin{aligned} \hat{I}_{2D} =& \hat{D}_{1-2}(\theta)\hat{I}_2\hat{D}^\dagger_{1-2}(\theta) \\ =& \hat{\sigma}_z + \left[\hat{a}^\dagger_1(\cos(\theta) - \sin(\theta)) + \hat{a}^\dagger_2(\cos(\theta) + \sin(\theta))\right][\text{H.c.}], \end{aligned} \tag{A6}$$

$$\hat{A}_{2D} = \hat{D}_{1-2}(\theta)\hat{A}_2\hat{D}^\dagger_{1-2}(\theta) = \frac{\hat{\sigma}_+(\hat{a}_1(\cos(\theta) - \sin(\theta)) + \hat{a}_2(\cos(\theta) + \sin(\theta)))}{\sqrt{\hat{I}_{2D} + 1}}, \tag{A7}$$

$$\hat{A}^\dagger_{2D} = \hat{D}_{1-2}(\theta)\hat{A}^\dagger_2\hat{D}^\dagger_{1-2}(\theta) = \frac{\hat{\sigma}_-\left(\hat{a}^\dagger_1(\cos(\theta) - \sin(\theta)) + \hat{a}^\dagger_2(\cos(\theta) + \sin(\theta))\right)}{\sqrt{\hat{I}_{2D} + 1}}. \tag{A8}$$

Therefore, the Hamiltonian in the new frame can be written as

$$\begin{aligned} \hat{H}_D =& \omega_F\hat{I}_1 + g\sqrt{\hat{I}_{2D} + 1}\left(\hat{A}_{2D} + \hat{A}^\dagger_{2D}\right) \\ =& \omega_F\hat{I}_1 + g\hat{\sigma}_+(\hat{a}_1(\cos(\theta) - \sin(\theta)) + \hat{a}_2(\cos(\theta) + \sin(\theta))) \\ &+ g\hat{\sigma}_-\left(\hat{a}^\dagger_1(\cos(\theta) - \sin(\theta)) + \hat{a}^\dagger_2(\cos(\theta) + \sin(\theta))\right), \end{aligned} \tag{A9}$$

which is given by Equation (16).

Appendix B.2. $N = 3$

For the three–field case, under the action of the transformation $\hat{D}_{1-3}(\theta)$, the operators $\hat{a}_1$, $\hat{a}_2$, and $\hat{a}_3$ transform as follows:

$$\hat{D}_{1-3}(\theta)\hat{a}_1\hat{D}^{\dagger}_{1-3}(\theta) = \hat{a}_1\cos(\theta) + \frac{\hat{a}_2+\hat{a}_3}{\sqrt{2}}\sin(\theta), \tag{A10}$$

$$\hat{D}_{1-3}(\theta)\hat{a}_2\hat{D}^{\dagger}_{1-3}(\theta) = \hat{a}_2 - \frac{\hat{a}_1}{\sqrt{2}}\sin(\theta) + \frac{\hat{a}_2+\hat{a}_3}{2}(\cos(\theta)-1), \tag{A11}$$

$$\hat{D}_{1-3}(\theta)\hat{a}_3\hat{D}^{\dagger}_{1-3}(\theta) = \hat{a}_3 - \frac{\hat{a}_1}{\sqrt{2}}\sin(\theta) + \frac{\hat{a}_2+\hat{a}_3}{2}(\cos(\theta)-1). \tag{A12}$$

From these results, it follows that the invariants transform in the following way

$$\hat{I}_{1D} = \hat{D}_{1-3}(\theta)\hat{I}_1\hat{D}^{\dagger}_{1-3}(\theta) = \hat{I}_1, \tag{A13}$$

$$\begin{aligned}\hat{I}_{2D} =& \hat{D}_{1-3}(\theta)\hat{I}_2\hat{D}^{\dagger}_{1-3}(\theta)\\ =& \frac{3}{2}\hat{\sigma}_z + \left[\hat{a}_1^{\dagger}(\cos(\theta)-\sqrt{2}\sin(\theta)) + \hat{B}^{\dagger}_{2-3}(\sin(\theta)+\sqrt{2}\cos(\theta))\right][\text{H.c.}],\end{aligned} \tag{A14}$$

and the operator $\hat{A}_3$ is transformed as

$$\hat{A}_{3D} = \hat{D}_{1-3}(\theta)\hat{A}_3\hat{D}^{\dagger}_{1-3}(\theta) = \frac{\hat{\sigma}_+\left(\hat{a}_1(\cos(\theta)-\sqrt{2}\sin(\theta)) + \hat{B}_{2-3}(\sin(\theta)+\sqrt{2}\cos(\theta))\right)}{\sqrt{\hat{I}_{2D}+\frac{3}{2}}}. \tag{A15}$$

Finally, the Hamiltonian in the transformed frame takes the form given by Equation (33).

Appendix B.3. General Case for N Fields

We now generalize the previous cases by considering the interaction of N quantized fields with the atom. Under the action of the operator $\hat{D}_{1-N}(\theta)$, the annihilation operators corresponding to each field transform as follows:

$$\hat{D}_{1-N}(\theta)\hat{a}_1\hat{D}^{\dagger}_{1-N}(\theta) = \hat{a}_1\cos(\theta) + \hat{B}_{2-N}\sin(\theta), \tag{A16}$$

$$\hat{D}_{1-N}(\theta)\hat{a}_i\hat{D}^{\dagger}_{1-N}(\theta) = \hat{a}_i - \frac{\hat{a}_1}{\sqrt{N-1}}\sin(\theta) + \frac{\hat{B}_{2-N}}{\sqrt{N-1}}(\cos(\theta)-1), \tag{A17}$$

where $i = 2, 3, \ldots, N$. From these results, it follows that the invariants transform as

$$\hat{I}_{1D} = \hat{D}_{1-N}(\theta)\hat{I}_1\hat{D}^{\dagger}_{1-N}(\theta) = \hat{I}_1, \tag{A18}$$

$$\begin{aligned}\hat{I}_{2D} &= \hat{D}_{1-N}(\theta)\hat{I}_2\hat{D}^{\dagger}_{1-N}(\theta)\\ &= \frac{N}{2}\sigma_z + \left[\hat{a}_1^{\dagger}\left(\cos(\theta)-\sqrt{N-1}\sin(\theta)\right) + \hat{B}^{\dagger}_{2-N}\left(\sin(\theta)+\sqrt{N-1}\cos(\theta)\right)\right][\text{H.c.}],\end{aligned} \tag{A19}$$

and the operator $\hat{A}_N$ transforms as

$$\begin{aligned}\hat{A}_{ND} &= \hat{D}_{1-N}(\theta)\hat{A}_N\hat{D}^{\dagger}_{1-N}(\theta)\\ &= \frac{\sigma_+\left[\hat{a}_1\left(\cos(\theta)-\sqrt{N-1}\sin(\theta)\right) + \hat{B}_{2-N}\left(\sin(\theta)+\sqrt{N-1}\cos(\theta)\right)\right]}{\sqrt{\hat{I}_{2D}+\frac{N}{2}}}.\end{aligned} \tag{A20}$$

Therefore, using these expressions, the Hamiltonian of the system in the new reference frame can be written as given in Equation (51).

References

1. Rabi, I.I. Space Quantization in a Gyrating Magnetic Field. *Phys. Rev.* **1937**, *51*, 652–654. [CrossRef]
2. Braak, D. Integrability of the Rabi Model. *Phys. Rev. Lett.* **2011**, *107*, 100401. [CrossRef]
3. Jaynes, E.; Cummings, F. Comparison of quantum and semiclassical radiation theories with application to the beam maser. *Proc. IEEE* **1963**, *51*, 89–109. [CrossRef]
4. Shore, B.W.; Knight, P.L. The jaynes-cummings model. *J. Mod. Opt.* **1993**, *40*, 1195–1238.
5. Larson, J.; Mavrogordatos, T. *The Jaynes–Cummings Model and Its Descendants*; IOP Publishing: Bristol, UK, 2021; pp. 2053–2563. [CrossRef]
6. Eberly, J.H.; Narozhny, N.B.; Sanchez-Mondragon, J.J. Periodic Spontaneous Collapse and Revival in a Simple Quantum Model. *Phys. Rev. Lett.* **1980**, *44*, 1323–1326. [CrossRef]
7. Narozhny, N.B.; Sanchez-Mondragon, J.J.; Eberly, J.H. Coherence versus incoherence: Collapse and revival in a simple quantum model. *Phys. Rev. A* **1981**, *23*, 236–247. [CrossRef]
8. Meystre, P.; Zubairy, M. Squeezed states in the Jaynes-Cummings model. *Phys. Lett. A* **1982**, *89*, 390–392. [CrossRef]
9. Guo, G.C.; Zheng, S.B. Generation of Schrödinger cat states via the Jaynes-Cummings model with large detuning. *Phys. Lett. A* **1996**, *223*, 332–336. [CrossRef]
10. Anaya-Contreras, J.A.; Ramos-Prieto, I.; Zúñiga-Segundo, A.; Moya-Cessa, H.M. The anisotropic quantum Rabi model with diamagnetic term. *Front. Phys.* **2025**, *13*, 1568407. [CrossRef]
11. Campos-Uscanga, A.; Rodríguez, E.B.; Martínez, E.P.; Bastarrachea-Magnani, M.A. Magic States in the Asymmetric Quantum Rabi Model. *arXiv* **2025**, arXiv:2508.00765. [CrossRef]
12. Asbóth, J.K.; Domokos, P.; Ritsch, H. Correlated motion of two atoms trapped in a single-mode cavity field. *Phys. Rev. A* **2004**, *70*, 013414. [CrossRef]
13. Roversi, J.A.; Vidiella-Barranco, A.; Moya-Cessa, H. Dynamics of two atoms coupled to a cavity field. *Mod. Phys. Lett. B* **2003**, *17*, 219–224. [CrossRef]
14. Dicke, R.H. Coherence in Spontaneous Radiation Processes. *Phys. Rev.* **1954**, *93*, 99–110. [CrossRef]
15. Braak, D. Solution of the Dicke model for N = 3. *J. Phys. B At. Mol. Opt. Phys.* **2013**, *46*, 224007. [CrossRef]
16. Tavis, M.; Cummings, F.W. Exact Solution for an *N*-Molecule—Radiation-Field Hamiltonian. *Phys. Rev.* **1968**, *170*, 379–384. [CrossRef]
17. Abdel-Hafez, A.M.; Obada, A.S.F.; Ahmad, M.M.A. N-level atom and (N-1) modes: An exactly solvable model with detuning and multiphotons. *J. Phys. A Math. Gen.* **1987**, *20*, L359. [CrossRef]
18. Kochetov, E. A generalized N-level single-mode Jaynes-Cummings model. *Phys. A Stat. Mech. Its Appl.* **1988**, *150*, 280–292. [CrossRef]
19. Bužek, V. N-level Atom Interacting with Single-mode Radiation Field: An Exactly Solvable Model with Multiphoton Transitions and Intensity-dependent Coupling. *J. Mod. Opt.* **1990**, *37*, 1033–1053. [CrossRef]
20. Gerry, C.C. Conditional state generation in a dispersive atom-cavity field interaction with a continuous external pump field. *Phys. Rev. A* **2002**, *65*, 063801. [CrossRef]
21. Vidiella-Barranco, A.; Magalhães de Castro, A.S.; Sergi, A.; Roversi, J.A.; Messina, A.; Migliore, A. Analytical Solutions of the Driven Time-Dependent Jaynes–Cummings Model. *Ann. Phys.* **2025**, *537*, e00148. [CrossRef]
22. Bocanegra-Garay, I.A.; Hernández-Sánchez, L.; Ramos-Prieto, I.; Soto-Eguibar, F.; Moya-Cessa, H.M. Invariant approach to the driven Jaynes-Cummings model. *SciPost Phys.* **2024**, *16*, 007. [CrossRef]
23. Buck, B.; Sukumar, C. Exactly soluble model of atom-phonon coupling showing periodic decay and revival. *Phys. Lett. A* **1981**, *81*, 132–135. [CrossRef]
24. Sukumar, C.; Buck, B. Multi-phonon generalisation of the Jaynes-Cummings model. *Phys. Lett. A* **1981**, *83*, 211–213. [CrossRef]
25. Singh, S. Field statistics in some generalized Jaynes-Cummings models. *Phys. Rev. A* **1982**, *25*, 3206–3216. [CrossRef]
26. Tsutsui, T.T.; Cius, D.; Vidiella-Barranco, A.; de Castro, A.S.M.; Andrade, F.M. Revisiting the Jaynes–Cummings model with time-dependent coupling. *Braz. J. Phys.* **2026**, *56*, 21. [CrossRef]
27. Papadopoulos, G.J. Energetics of radiation and a two-level atom in an ideal resonant cavity. *Phys. Rev. A* **1988**, *37*, 2482–2487. [CrossRef]
28. Abdalla, M.; Ahmed, M.; Obada, A.S. Multimode and multiphoton processes in a non-linear Jaynes-Cummings model. *Phys. A Stat. Mech. Its Appl.* **1991**, *170*, 393–414. [CrossRef]
29. Wildfeuer, C.; Schiller, D.H. Generation of entangled N-photon states in a two-mode Jaynes-Cummings model. *Phys. Rev. A* **2003**, *67*, 053801. [CrossRef]
30. Abdalla, M.S.; Ahmed, M.M.A.; Obada, A.S.F. Some statistical properties of the interaction between a two-level atom and three field modes. *Laser Phys.* **2015**, *25*, 065204. [CrossRef]
31. Seke, J. Extended Jaynes–Cummings model. *J. Opt. Soc. Am. B* **1985**, *2*, 968–970. [CrossRef]

32. Dutra, S.M.; Knight, P.L.; Moya-Cessa, H. Discriminating field mixtures from macroscopic superpositions. *Phys. Rev. A* **1993**, *48*, 3168. [CrossRef]
33. Benivegna, G. Quantum effects in the transient dynamics of a many mode Jaynes-Cummings model. *J. Mod. Opt.* **1996**, *43*, 1589–1601. [CrossRef]
34. Larson, J. Scheme for generating entangled states of two field modes in a cavity. *J. Mod. Opt.* **2006**, *53*, 1867–1877. [CrossRef]
35. Benivegna, G.; Messina, A. New Quantum Effects in the Dynamics of a Two-mode Field Coupled to a Two-level Atom. *J. Mod. Opt.* **1994**, *41*, 907–925. [CrossRef]
36. Siegman, A.E. *Lasers*; University Science Books: Sausalito, CA, USA, 1986.
37. Saleh, B.E.A.; Teich, M.C. *Fundamentals of Photonics*, 3rd ed.; Wiley Series in Pure and Applied Optics; Wiley: Hoboken, NJ, USA, 2019.
38. Sakurai, J.J.; Napolitano, J. *Modern Quantum Mechanics*, 3rd ed.; Cambridge University Press: Cambridge, UK, 2020.
39. Wei, J.; Norman, E. On global representations of the solutions of linear differential equations as a product of exponentials. *Proc. Am. Math. Soc.* **1964**, *15*, 327–334. [CrossRef]
40. Campos, R.A.; Saleh, B.E.A.; Teich, M.C. Quantum-mechanical lossless beam splitter: SU(2) symmetry and photon statistics. *Phys. Rev. A* **1989**, *40*, 1371–1384. [CrossRef]
41. Gerry, C.; Knight, P. *Introductory Quantum Optics*; Cambridge University Press: Cambridge, UK, 2004.
42. Johansson, J.; Nation, P.; Nori, F. QuTiP 2: A Python framework for the dynamics of open quantum systems. *Comput. Phys. Commun.* **2013**, *184*, 1234–1240. [CrossRef]
43. Yeh, L. Ermakov-Lewis invariant from the Wigner function of a squeezed coherent state. *Phys. Rev. A* **1993**, *47*, 3587–3592. [CrossRef]

Disclaimer/Publisher's Note: The statements, opinions and data contained in all publications are solely those of the individual author(s) and contributor(s) and not of MDPI and/or the editor(s). MDPI and/or the editor(s) disclaim responsibility for any injury to people or property resulting from any ideas, methods, instructions or products referred to in the content.